PAPER

Check for updates

Divalent cation effects in the glass transition of poly(diallyldimethylammonium)–poly(styrene sulfonate) polyelectrolyte complexes†

Tamunoemi Braide,[a] Suvesh Manoj Lalwani,[a] Chikaodinaka I. Eneh[a] and Jodie L. Lutkenhaus [ID] *[ab]

The assembly and dynamics of polyelectrolyte complexes (PECs) and polyelectrolyte multilayers (PEMs) are influenced by water content, pH, and salt concentration. However, the influence of divalent salts on the assembly of polyelectrolyte complexes remains unclear. This work showcases that divalent chloride salts directly impact the glass transition temperature and the ion–ion interactions within PECs. Here, poly(diallyldimethylammonium)–poly(styrene sulfonate) (PDADMA–PSS) PECs are assembled in solutions containing $MgCl_2$ and $CaCl_2$ (following the Hofmeister series). These PECs are studied for the cations' influence on physicochemical properties (glass transition, polymer composition, ion pairing) at varying salt concentrations (0.03 M, 0.10 M, 0.15 M, and 0.20 M). Modulated differential scanning calorimetry (MDSC) experiments demonstrate that PECs assembled with $CaCl_2$ have a significantly higher glass transition temperature when compared to PECs assembled with $MgCl_2$. Neutron activation analysis (NAA) and nuclear magnetic resonance (NMR) spectroscopy demonstrate that this difference is due to strong ion-specific effects influencing the ratio of intrinsic and extrinsic ion pairings in the system. Furthermore, this study demonstrates a universal linear relationship between the thermal transition and the number of water molecules surrounding oppositely charged polyelectrolyte–polyelectrolyte intrinsic ion pairs, even when the salt contains divalent cations. Ion-specific trends have implications on the glass transition and composition of PDADMA–PSS PECs. Divalent salts not only follow the trend of the Hofmeister series but also introduce bridging into the polyelectrolyte complex; however, the structural relaxation of the PEC remains the same. This study offers a bridge between divalent cation behavior on polymer assembly properties and its transition to industrial applications such as controlled drug delivery, sensors, and water purification.

1. Introduction

Polyelectrolyte complexes (PECs) and polyelectrolyte multilayers (PEMs) are formed by the entropic release of counterions and solvent from the polyelectrolyte charge groups, followed by electrostatic interactions in a polar solvent to form polymer-rich (complex) and polymer-deficient (supernatant) phases.[1–4] As a result, polyelectrolyte assemblies have vast applications in water treatment, saloplastics, bioelectronics, hydrogels, antimicrobial coatings, batteries, additives in cosmetics and detergents, and drug delivery systems.[5–11] Previous works have reported extensively on the influence of the water content,[12–14] pH,[13] charge density,[15,16] temperature,[17] and polyelectrolyte molecular weight[18,19] on PECs and PEMs.[12–14] However, the influence of multivalent salts on the composition and thermal properties of polymer assemblies needs a deeper understanding.

When oppositely charged polyelectrolytes associate, intrinsic ion pairs form between polycation and polyanion charge groups.[20–24] Extrinsic ion pairs can also form between the polyelectrolyte charge groups and counterions in the system. Increasing the salt concentration promotes charge screening, thus increasing the fraction of extrinsic ion pairs in the system. As a result of increased salt concentration, complexes can exhibit decreased viscosity and even decomplexation.[25] Salt concentration can also influence whether a solid or liquid PEC phase forms.[26]

Besides salt concentration, the amount of water in the isolated complex can also influence its macromolecular properties. Michaels *et al.* first described water as a plasticizer of

[a] Artie McFerrin Department of Chemical Engineering, Texas A&M University, College Station, Texas 77840, USA. E-mail: jodie.lutkenhaus@tamu.edu

[b] Department of Materials Science and Engineering, Texas A&M University, College Station, Texas 77840, USA

† Electronic supplementary information (ESI) available. See DOI: https://doi.org/10.1039/d4sm00856a

PECs.[27] Lyu *et al.*[28] also reported the plasticizing effects of water on poly(diallyldimethylammonium)–poly(styrene sulfonate) (PDADMA–PSS) complex fibers at different relative humidities. This work compared changes in the elastic storage modulus for PECs stored under ambient and dry conditions. Elsewhere, De *et al.*[29] showed the variation of ionic conductivity with humidity for PDADMA–PSS PECs, in which ion transport increased with hydration as water facilitates ion diffusion within the complex.

In our own group, we have extensively explored how water and salt affect intrinsic ion pairing and the glass transition of solid-like PEMs and PECs.[13,14,30–34] Specifically, a scaling relationship for water, intrinsic ion pairing, and the glass transition was established:[14]

$$\ln\left(n_{H_2O}\big/n_{intrinsic\ ion\ pair}\right) \propto T_g^{-1} \tag{1}$$

Using eqn (1), the water–salt–temperature dependence for PDADMA/PSS PECs and PEMs with NaCl showed a collapse and linearization of T_g values for a NaCl concentration range of 0–1.5 M.[14] Our group showed that the addition of water leads to softer complexes and that the addition of salt introduces screening effects and breaks down intrinsic ion pairing – both of which lower the complex's T_g.[31] In studies on PDADMA/PSS PEMs, we showed that NaCl and KBr dope the PEMs with different degrees of efficacy.[30,34] Specifically, KBr was a better dopant than NaCl, characterized by higher levels of swelling in PEMs assembled and exposed to KBr. The T_g response followed that of eqn (1) for both NaCl and KBr, but distinct differences were observed. Specifically, the slopes for the linear fits were the same, but the *y*-intercepts were different for the PEMs assembled in the two different salts. We interpreted the slope as a Van't Hoff enthalpy associated with the insertion/de-insertion of a water molecule in the intrinsic ion pair's hydration shell, and the *y*-intercept has been interpreted as an entropic contribution.[33] Our recent work investigated anion $(Cl^-, Br^-, NO_3^-, I^-)$ effects on the T_g in which the relative chao/kosmotropic nature of the anion played an important role.[35] The role of multivalent cations on the glass transition of PECs has yet to be explored, and it is unclear if the response will follow eqn (1) or if the results can be interpreted in the same manner.

Multivalent ions can interact with two (for divalent ions) or three (for trivalent ions) charged groups on a complementary polyion. This phenomenon is termed "bridging", and it is a form of physical crosslinking that introduces changes in mechanical properties and coacervation.[36–40] Bridging can exist between the same polymer chain (intramolecular) and/or between two polymer chains (inter-molecular); depending on which type of bridging dominates, the properties of the resulting polymer can be affected.[41] A handful of studies have explored how multivalent cations influence PEC composition and phase separation. For example, Iyer *et al.*[39] highlighted the significant impact of divalent (Ca^{2+}, Sr^{2+}) ions on poly(allylamine hydrochloride)–poly(acrylic acid) (PAH–PAA) complexes. Divalent ions preferentially partitioned into the complex phase as compared to monovalent ions. The authors also found that introducing divalent counterions influenced the viscoelastic properties of the PEC through bridging effects which hindered chain relaxation. Perry *et al.*[42] studied the effect of salt ion valency on the coacervation of vinyl polyelectrolytes using turbidity measurements. The authors noted that divalent cations suppressed coacervation to a greater extent than monovalent cations. This was linked to the Hofmeister series placement in which $CaCl_2$ suppressed coacervation more than NaCl due to Ca^{2+} being more chaotropic than Na^+, favoring "salting-in" and increasing polymer solubility.[42] Dautzenberg and Kriz[40] also studied dissimilarities in the stability and aggregation behavior of PECs with multivalent salts $(CaCl_2, MgCl_2, FeCl_3, AlCl_3)$ *versus* NaCl. Notably, the authors showed that the ion radius of monovalent cations did not affect the response of the complex particles. Taken together, multivalent ions significantly impact the physical and mechanical properties of polyelectrolyte complexes and multilayers alike because the multivalent ion can interact with more than one charge group.

Multivalent ion – homopolymer mixtures can inform our understanding of the nature of multivalent ions in PECs. For example, PSS brushes exposed to different divalent counterions shrank following a trend with the ionic radius, $Mg^{2+} < Ca^{2+} < Ba^{2+}$.[37] The authors ascribed this trend to the binding enthalpy's decrease with increasing ionic radius. Sinn *et al.*[43] studied the binding of Ca^{2+} to PAA and established that entropic effects, not electrostatic force, is the primary reason for the stronger binding of multivalent ions to PAA. Chen *et al.*[44] established an affinity sequence for different cations with PSS as $Ba^{2+} > Pb^{2+} > Sr^{2+} > Ca^{2+} > Cu^{2+} > Mg^{2+} > H^+ > K^+ > Na^+ > Li^+$. The authors applied Pauley's model,[45] which predicts cation-exchange equilibria to show that selectivity is a function of ionic radius for ionic complexation. In sum, multivalent cations exhibit varying strengths of binding with a polyanion, leading us to hypothesize that this effect may influence the glass transition in PECs.

Here, we explore the effects of salts containing divalent cations on the hydration, composition, and glass transition temperature of PDADMA–PSS PECs. Specifically, solid PECs are prepared from aqueous mixtures of varying concentrations of NaCl, $CaCl_2$, and $MgCl_2$, for which NaCl serves as a comparison for monovalent *vs.* divalent cation behavior. The glass transition was quantified using modulated differential scanning calorimetry (MDSC) of PECs hydrated with varying amounts of solution (20–26 wt%). The compositions of the PECs were determined using proton nuclear magnetic resonance (^{1}H NMR) spectroscopy and neutron activation analysis (NAA). Together, this information allows for the comparison of the glass transition temperature with respect to intrinsic ion pairing, hydration, and bridging caused by the divalent cation.

2. Experimental section

2.1. Materials

Poly(diallyldimethylammonium) (PDADMA, M_w = 200 000–350 000 g mol^{-1}, 20 wt% solution) and poly(styrene sulfonate)

(PSS, M_w = 500 000 g mol^{-1}) were purchased from Polysciences, Inc. and their structures are shown in Fig. 1 below. The salts used, calcium chloride ($\geq$96.0%) and magnesium chloride ($\geq$98.0%), were purchased from Sigma Life Sciences. Deuterium oxide (D$_2$O) (99.8% deuterium) used in H-NMR spectroscopy was purchased from Tokyo Chemical Industries Co. Milli-Q water was used in all experiments.

2.2. Polyelectrolyte complex preparation

80 mL solutions of 50 mM PDADMA and PSS were prepared with respect to their repeating unit molar mass. Depending on the system, the desired salt type (NaCl, CaCl$_2$, and MgCl$_2$) and concentration (0.03–0.20 M) were introduced during assembly. Once the solutions were fully mixed with the salt, the PDADMA solution was quickly added to the PSS solution and stirred for 30 minutes at 600 rpm. The mixture was then centrifuged at 10 000 rpm for 10 min. The complex was collected, pressed using a Carver Press at 6000 psi, extensively rinsed with Milli-Q water, and dried in a convection oven overnight at 343 K. The dried PECs were ground into a fine powder, dried under vacuum for 6 h at 423 K, and then sealed in an airtight container until further characterization.

2.3. Modulated differential scanning calorimetry (MDSC)

Modulated DSC measurements were performed on the dried PECs using a TA Q200 differential scanning calorimeter to measure the glass transition temperature of the hydrated polymers. The dried polymers were hydrated using the solution corresponding to the salts added during assembly, i.e., the dried PDADMA–PSS PECs prepared with 0.10 M CaCl$_2$ were hydrated with a 0.10 M CaCl$_2$ solution. This procedure minimizes any change in the PEC's ion pairing and allows us to assume that the original PEC remains of identical composition to the one tested in the DSC pan. The PECs were prepared at varying hydration levels (20, 22, 24, 26 wt%) in T-zero aluminum pans (TA instruments), with hydrated sample masses ranging from 7–12 mg. Once hydrated and sealed with a hermetic lid (TA instruments), the samples were left to equilibrate for 24 hours before testing. Measurements were performed in a heat–cool–heat–cool cycle. The samples were heated from 273 K to 278 K and held isothermally for 5 min, followed by a ramp to 393 K at a rate of 2 K min^{-1} and an amplitude of 1.272 K for a period of 60 s. The cooling cycle

involved lowering the temperature of the sample from 393 K back to 278 K at the same rate. Nitrogen was used as the purge gas at 50 mL min^{-1}. The MDSC thermograms are shown in exotherm down, and the inflection point of the second heating cycle was recorded as the glass transition temperature. The measurements were taken in triplicates, and standard deviations were obtained.

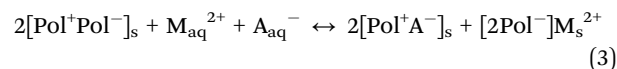## 2.4. Proton nuclear magnetic resonance (^{1}H NMR) spectroscopy

The composition of the PECs was measured using proton nuclear magnetic resonance spectroscopy (500 MHz proton, Varian Inova 500 spectrometer). 30 mg of the dried PEC was dissolved in 0.7 mL of 2.5 M potassium bromide (KBr) in deuterium oxide (D$_2$O) and then transferred to an NMR tube. The NMR spectra were collected, and the D$_2$O solvent peak was used as a reference point at 4.79 ppm to calculate the composition of PDADMA and PSS in the polymer complex. The compositions were calculated by integrating the area under the peaks from the spectra to obtain the four aromatic hydrogens of PSS (5.5–9 ppm) and the nineteen aliphatic hydrogens (sixteen from PDADMA and three from PSS) (0–4.6 ppm). The following equation was then used to calculate the PSS/PDADMA ratio in the complex:

$$\frac{\text{PSS}}{\text{PDADMA}} = \frac{4A_{\text{aromatic}}}{A_{\text{aliphatic}} - \frac{3}{4}(A_{\text{aromatic}})} \tag{2}$$

2.5. Neutron activation analysis (NAA)

NAA was used for elemental analysis of the dried PEC samples. For CaCl$_2$-PECs, the samples were tested for Na, S, Cl, and Ca. For MgCl$_2$-PECs, the elements tested were Na, S, Cl, and Mg. In this system, PDADMA contributes nitrogen and a portion of chlorine, PSS contributes sulfur and sodium, and the rest of the ions are from the assembly conditions.

For our calculations, we assumed that the counterions were paired with a complementary polyelectrolyte as an extrinsic ion pair (i.e., there are no co-ions). The possible different types of ion-polyelectrolyte pairings are shown in Fig. S1 and S2 (ESI†). Eqn (3) shows one example, in which intrinsic ion pairs between the oppositely charged poly-ions [Pol$^+$Pol$^-$]$_s$) are disrupted with a divalent cation and two monovalent anions to generate extrinsic ion pairings: two pairs of a polycation repeat unit-monovalent anion (2[Pol$^+$A$^-$]) and one of a divalent cation with two polyanion repeat units ([2Pol$^+$]M^{2+}).

$$2[\text{Pol}^+\text{Pol}^-]_s + M_{aq}^{2+} + A_{aq}^- \leftrightarrow 2[\text{Pol}^+\text{A}^-]_s + [2\text{Pol}^-]M_s^{2+} \tag{3}$$

To calculate the number of moles of extrinsic and intrinsic ion pairs in a PEC sample, and hence the doping level, we used the ion compositions from NAA. For monovalent ions (i.e., Na$^+$ and Cl$^-$) the various ion–ion interactions possible in the system were calculated by the following expressions:
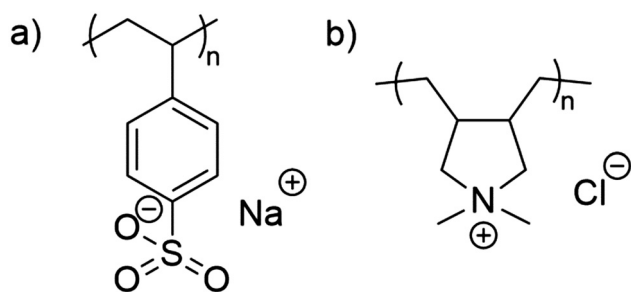

Fig. 1 Structures of polyelectrolytes used in this study. (a) Poly(styrene sulfonate) (PSS) and (b) poly(diallyldimethylammonium) (PDADMA).

$$n_{\text{PSS–Na}} = n_{\text{Na}}$$

$$n_{\text{PSS–PDADMA}} = n_{\text{S}} - n_{\text{PSS–Na}}$$

$$n_{\text{PDADMA–Cl}} = n_{\text{Cl}} \qquad (4\text{a–c})$$

In a divalent system, MCl_2, the divalency of the cation must be taken into consideration. Further, PECs made from sodium-containing PSS will exhibit residual traces of sodium, even if assembled in a divalent salt. These considerations lead to a new set of equations, where the sodium and divalent cation concentrations are obtained from NAA:

$$n_{\text{PSS–Na}} = n_{\text{Na}}$$

$$n_{\text{PSS–M}} = 2n_{\text{M}}$$

$$n_{\text{PSS–PDADMA}} = n_{\text{S}} - (n_{\text{PSS–Na}} + n_{\text{PSS–M}})$$

$$n_{\text{PDADMA–Cl}} = n_{\text{Cl}} \qquad (5\text{a–d})$$

The moles of PSS–PDADMA intrinsic pairs, $n_{\text{PSS–PDADMA}}$, is calculated on a 100 g PEC basis. The equation and sample calculation are below.

$$n_{\text{intrinsic ion pair}} = \frac{\text{actual mass of PEC (g)} \times n_{\text{PSS–PDADMA}} \text{(mol)}}{100 \text{ (g)}} \qquad (6)$$

The actual mass of PEC and the hydration level are obtained from MDSC. For example, consider 100 g of a 0.15 M $CaCl_2$-PEC with a hydration level of 20.15 wt%. The mass of the PEC is 100 g − 20.15 g = 79.85 g, from NAA and eqn (5), $n_{\text{PSS–PDADMA}} = 0.231$ mol.

$$n_{\text{intrinsic ion pair}} = \frac{79.850 \text{ g} \times 0.231 \text{ mol}}{100 \text{ g}} = 0.184 \text{ mol}$$

The moles of the ion pairs and the concentrations can be used interchangeably because they are all present within the same PEC volume. The calculation of doping levels is described in the Results and discussion section.

3. Results and discussion

PDADMA and PSS solutions were prepared at concentrations of 50 mM with respect to their repeating unit. The separate solutions were mixed with varying salt types (NaCl, $CaCl_2$, and $MgCl_2$) and concentrations (0.03–0.20 M). Then, the polycation and polyanion solutions were combined to form a cloudy white product. Here, we refer to the PEC and its type of salt during assembly as "salt-PEC"; for example, "$CaCl_2$-PEC" denotes a PEC assembled from $CaCl_2$-containing solutions. The resulting solid PEC product was isolated using centrifugation, rinsed extensively, dried, and crushed into a powder for further characterization. These salt concentrations were chosen based on our observations of polymer solubility. Specifically, PSS solutions became cloudy when the $CaCl_2$ concentration was greater than 0.25 M. Elsewhere, it has been shown that PSS has

a high affinity for multivalent cations such as Ca^{2+} and Mg^{2+} and can form complexes or even precipitates with them.[44,46]

3.1. Effect of salt type on the composition and stoichiometry of PDADMA–PSS PECs

NAA measurements, which reveal the weight percentages of elements Na, S, N, Cl, Ca, and Mg, were collected for $CaCl_2$-PECs and $MgCl_2$-PECs prepared from varying salt concentrations (Tables S1 and S2, ESI†). From this information, the doping level of the polymers can be estimated, as shown in Fig. 2 and Table S5 (ESI†). We assumed that each Cl^- ion was associated with one extrinsic PDADMA site and that each divalent cation was associated with two extrinsic PSS sites. This assumption excludes the possibility of co-ions, which are ions within the complex that are unassociated with either of the polyelectrolytes. The doping level, y, which reflects the fraction of polyelectrolyte charge groups that are extrinsically
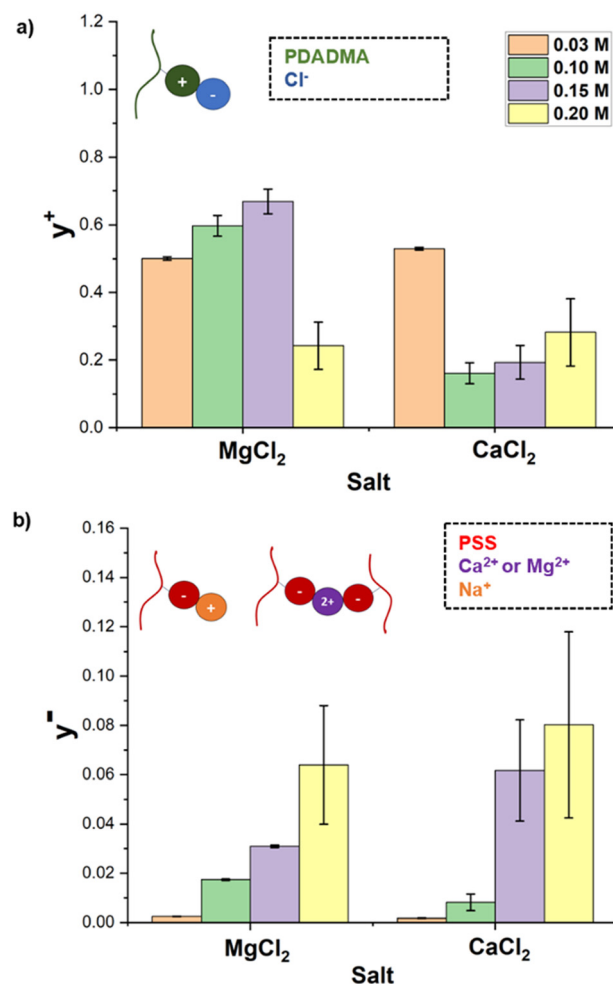

Fig. 2 Cationic and anion doping levels for PDADMA–PSS PECs prepared with varying concentrations of $MgCl_2$ and $CaCl_2$ (a) PDADMA doping level (y^+) and (b) PSS doping level (y^-). Here y^- and y^+ are calculated using eqn (2) and associated NAA data in Tables S1 and S2 (ESI†). The legend in (a) applies to panel (b).

compensated,[47] can be described as cationic (y^+) and anionic (y^-) doping levels, as shown below:

$$y^+ = \frac{[Cl^-]}{[PDADMA]}, \quad y^- = \frac{[M^{2+}] + 2[Na^+]}{2[PSS]} \quad (7)$$

where $[Cl^-]$, $[M^{2+}]$, and $[Na^+]$ represent the concentrations of the respective monovalent and divalent ions and $[PDADMA]$ and $[PSS]$ represent the concentrations of polyelectrolyte repeat units. The concentration of sodium ions is included in eqn (7) because small amounts of Na^+ were sometimes detected.

The cationic and anionic doping levels, y^+ and y^-, were calculated for CaCl$_2$-PECs and MgCl$_2$-PECs prepared from varying salt concentrations (0.03, 0.10, 0.15, and 0.20 M). As shown in Fig. 2a, at 0.03 M MgCl$_2$, 50% of PDADMA units interact with chloride ions, peaking at 67% for 0.15 M and falling to 24% at 0.20 M. For CaCl$_2$-PECs, y^+ peaks at 0.03 M (53% of PDADMA units), drops at 0.10 M, and rises with increasing concentrations. Instead, Fig. 2b shows that y^- monotonically increases with salt concentration for both systems. With y^+ being greater than y^- for all PECs examined, PDADMA exhibits consistently higher doping values than PSS. Additionally, CaCl$_2$-PECs show slightly higher doping levels compared to MgCl$_2$-PECs. For reference, y^+ and y^- for 0.1 M NaCl-PECs from Zhang et al.[14] were 0.16 and 0.01, respectively.

The trend in y^+ with increasing salt concentration may result from a competition between Coulomb screening and counter-ion binding effects.[48–50] Fig. 2a shows this transition occurs at 0.15–0.20 M for MgCl$_2$-PECs and 0.03–0.10 M for CaCl$_2$-PECs. Sadman et al.[51] and Yu et al.[37] described that divalent ions such as Ca^{2+} cause structural changes at low concentrations through bridging more effectively than Mg^{2+}. This explains why the transition concentration occurs at a lower salt concentration in CaCl$_2$-PECs. The lower PSS doping level (y^-) compared to PDADMA (y^+) is due to the excess PDADMA in the complex, with most PSS charge groups forming intrinsic ion pairs. This observation aligns with Jusufi et al.'s[48] findings on anionic sodium dodecyl sulfate (SDS) and cationic dodecyltrimethylammonium chloride (DTAC) systems.

Next, ^{1}H-NMR spectroscopy was used to determine the PSS ratio in the PECs, with Table S3 (ESI†) showing that CaCl$_2$-PECs and MgCl$_2$-PECs at 0.10 M had a PSS mol% of 47 ± 1 mol%. Varying the salt concentrations of assembly (0.03–0.20 M) had no major influence on the PEC's percentage of PSS (46–47 mol%). The higher y^+ values for PDADMA are explained by its excess in the PEC, where PSS cannot fully neutralize PDADMA, leading to asymmetric stoichiometry.

3.2. Effect of salt type on the hydration of PDADMA/PSS PECs

MDSC allows for the quantification of the glass transition in the divalent systems studied in this work. The glass transition is recorded as the inflection point of the reversible heat flow curve from the second heating cycle for PECs that were dried and then re-hydrated with a controlled amount of solution. Specifically, the PECs were re-hydrated with a solution that matched the complexation condition (i.e., a 0.20 M MgCl$_2$-PEC was rehydrated with a controlled volume of 0.20 M MgCl$_2$ aqueous
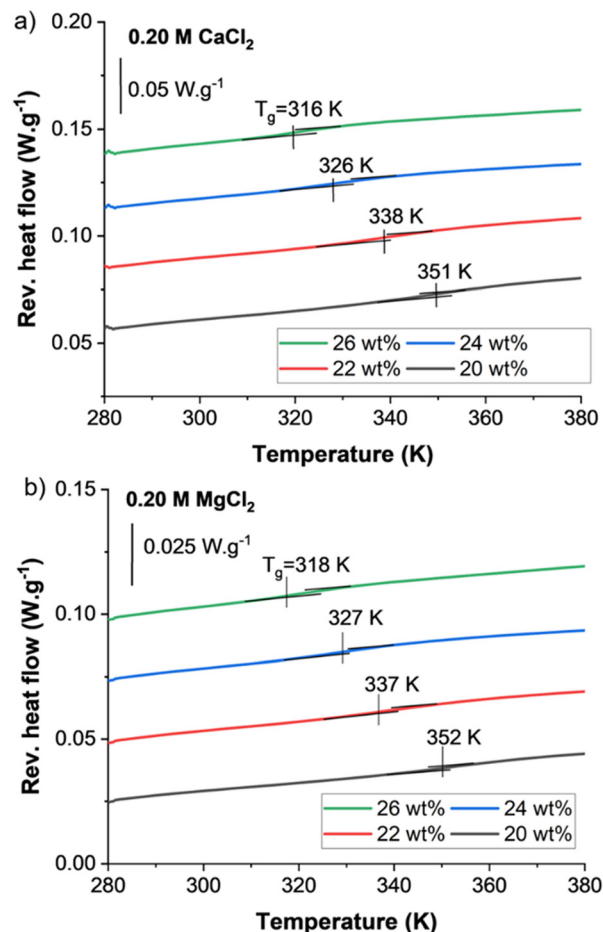

Fig. 3 MDSC Reversing heat flow curves for PDADMA–PSS PECs showing the glass transition from the second heating cycle for (a) 0.20 M CaCl$_2$ and (b) 0.20 M MgCl$_2$ PECs at varying water content (20–26 wt% added water). Curves shifted across the y-axis by a 20% gap for clarity. Exotherm down.

solution). As illustrated in Fig. 3a, for a fixed complexation salt concentration of 0.20 M, the T_g decreased from 351 to 316 K as the water content increased from 20 to 26 wt% for the 0.20 M CaCl$_2$-PEC. In comparison, Fig. 3b shows similar T_g-values for MgCl$_2$-PECs at equivalent hydrations. As described later, we found more variation in T_g-values between the PECs prepared in the two salts at other salt concentrations.

The decrease in a PEC's T_g with increasing hydration is expected and observed elsewhere in PDADMA–PSS PECs prepared from monovalent salts.[14] Water lubricates the polymer chains by decreasing the internal resistance of the polymer sliding motion.[52,53] Water also decreases the electrostatic attractions between polyelectrolyte intrinsic ion pairs and increases the free volume that facilitates polymer chain motion.[31,54,55] Taken together, the results in Fig. 3 confirm the same trend for divalent salt systems.

3.3. Effect of cation type on the glass transition of PDADMA/ PSS PECs

To study the effect of monovalent and divalent cations on the glass transition temperature of PDADMA–PSS PECs, NaCl,

CaCl$_2$, and MgCl$_2$ salts at the same ionic strength were studied at varying water content (20–26 wt%) using MDSC. This water content range was studied because the T_g was unobservable for water content levels below 20 wt% and above 26 wt%. Fig. 4 shows that at the same molarity and hydration of 0.10 M and 20 wt%, respectively, the NaCl-PECs had the highest T_g at 363 K, followed by CaCl$_2$-PECs at 349.6 K, and then MgCl$_2$ at 324.4 K. This ranking was consistent across all of the studied hydration levels.

Fig. 4 shows that the identity of the cation can strongly influence the PEC's T_g. One explanation for the varying T_g with salt type is the doping level. Fig. 2 shows that PECs prepared from MgCl$_2$ have slightly higher y^+ doping levels with PDADMA than those prepared from CaCl$_2$, which suggests more effective counterion binding and charge screening. This screening reduces Coulombic interactions within the PDADMA–PSS network, leading to increased chain mobility, which typically correlates with a lower T_g. This would lead to the expectation that MgCl$_2$-PECs would have lower T_g's than CaCl$_2$-PECs, as confirmed by Fig. 4.

Another explanation for the T_g trend in Fig. 4 lies in the varying cation–water interaction strengths, which are described qualitatively by the Jones-Dole B-coefficient, Table S4 (ESI†). This coefficient relates variations in an aqueous solution's viscosity to the ionic strength of a particular salt type. An increase in the Jones-Dole B-coefficient means stronger ion–water interactions in the solution,[56] for which the Jones-Dole B-coefficient is ranked as: Mg^{2+} > Ca^{2+} > Na$^+$. For comparison at 0.10 M, the PEC's glass transition temperature was lowest when prepared from MgCl$_2$ and highest for NaCl. Here, magnesium has: (1) the strongest interaction with water,[57] (2) the

largest hydrated radius,[58] and (3) the largest hydration number[57,59] of the three cations compared. One may also consider the ionic radius of the two ions. Mg^{2+}, with its smaller ionic radius and higher charge density compared to Ca^{2+}, can bind more strongly to the polyelectrolyte chains and weaken polycation–polyanion electrostatic interactions, which lowers the rigidity of the complex and reduces T_g. Ca^{2+}, on the other hand, being larger and less densely charged, may bind less efficiently, resulting in stronger residual Coulombic interactions and a comparatively higher T_g. We note that despite the hydration shell in MgCl$_2$-PECs limiting direct polymer binding, the higher charge density of Mg allows it to strongly polarize its local environment and screen electrostatic interactions with the polymer chains. This increases chain mobility and reduces the T_g. On the other hand, Ca, with its larger size and lower charge density, sheds its hydration shell more easily and forms stronger site-specific bridging interactions that stiffen the polymer matrix and increase T_g.

Separately, we also examined 0.30 M NaCl-PECs to compare the T_g for equivalent ionic strengths with 0.10 M CaCl$_2$-PECs and 0.10 M MgCl$_2$-PECs in Fig. S3 (ESI†). For 0.30 M NaCl-PECs, the complexes exhibited a higher doping level due to the higher salt concentration, thus lowering the T_g relative to 0.10 M NaCl-PECs.

3.4. Effect of ionic strength of divalent salts on the glass transition of PDADMA–PSS PECs

To understand the effect of salt concentration on the T_g of PDADMA–PSS PECs. The PECs were prepared using 0.03, 0.10, 0.15, and 0.20 M solutions of CaCl$_2$ and MgCl$_2$, and the T_g's were collected using MDSC as before. Fig. 5 compares the T_g at different hydration levels and salt concentrations for CaCl$_2$-PECs and MgCl$_2$-PECs.

In Fig. 5a, the T_g values were similar, regardless of salt concentration, for higher levels of hydration (24–26 wt%). However, at lower hydration levels (20–22 wt%) there is a spread in T_g values without a clear trend in salt concentration. This spread suggests that, with less water present, the effect of divalent counterions on the mobility of the PECs become more influential. This spread in T_g is more pronounced in Fig. 5b, for MgCl$_2$-PECs. Specifically, Fig. 5b shows that MgCl$_2$-PECs exhibit limited T_g overlap from 0.10 M to 0.20 M with clear partitioning at 0.03 M.

Divalent cations can interact with polyanions through bridging, coordinating with two negatively charged groups,[37,43,44,60,61] which may explain the spread in the T_g with salt concentration. Wei et al.[62] studied PDADMA/PSS multilayers exposed to Cu(NO$_3$)$_2$ and observed bridging at low concentrations (0.01 M), which led to film stiffening and de-swelling. At higher Cu(NO$_3$)$_2$ concentrations (0.03 M), swelling and softening occurred from disrupted ion pairs. This study highlights that bridging effects are more prominent at low concentrations. Glisman et al.[63] also demonstrated that Ca^{2+} bridging with PAA varies with salt concentration. PAA–Ca–PAA bridging is highest at low Ca^{2+} levels, while single PAA–Ca interactions dominate at higher concentrations due to chelation and "salting in" effects. As Fig. 4 shows, the PEC doping levels vary,
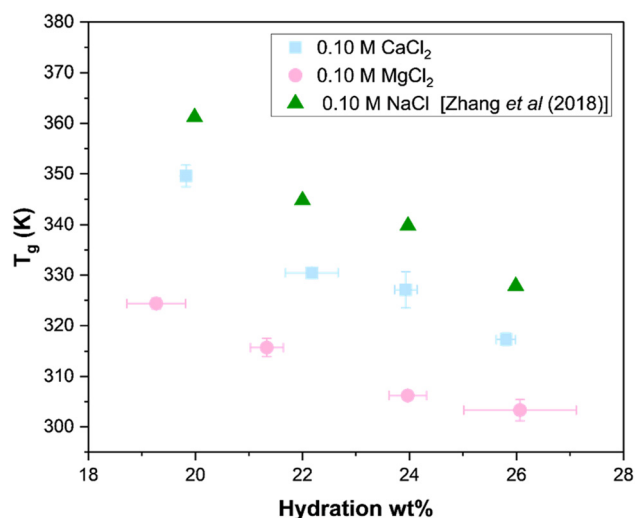

Fig. 4 Glass transition temperatures of PDADMA–PSS PECs prepared from NaCl, CaCl$_2$, or MgCl$_2$ solutions. The isolated PECs were rehydrated with a solution matching that of its assembly and examined using MDSC. 0.10 M NaCl reproduced with permissions from ref. 14 "Molecular Origin of the Glass Transition in Polyelectrolyte Assemblies." By Y. Zhang; P. Batys; J. T. O'Neal; F. Li; M. Sammalkorpi; J. L. Lutkenhaus, 2018. *ACS Central Sci.*, 4(5), 638–644. Copyright (2018) American Chemical Society.
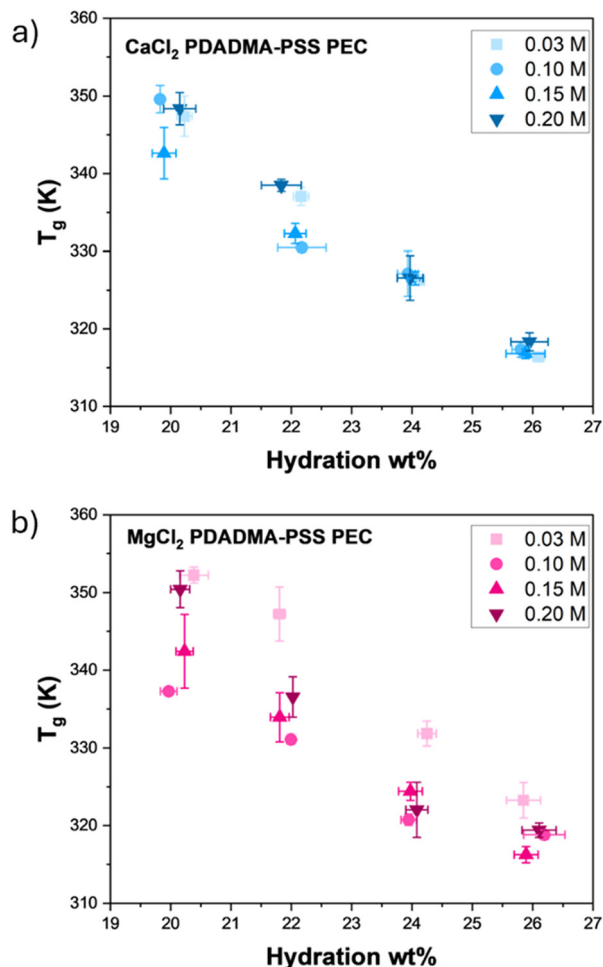
Fig. 5 Glass transition temperatures of PDADMA–PSS PECs prepared from solutions of varying (a) CaCl$_2$ or (b) MgCl$_2$ concentrations (0.03–0.20 M). The isolated PECs were rehydrated with a solution matching that of its assembly and examined using MDSC.

Fig. 6 Linear fitting of $\ln\left(\frac{n_{H_2O}}{n_{\text{intrinsic ion pair}}}\right)$ vs. $\frac{1000}{T_g}$ for PDADMA–PSS PEC systems of varying salt concentrations (0.03–0.20 M) of CaCl$_2$ and MgCl$_2$ with NaCl as a control. The data for PDADMA–PSS PECs at 0.10 M NaCl were reproduced with permission from ref. 14 "Molecular Origin of the Glass Transition in Polyelectrolyte Assemblies." By Y. Zhang; P. Batys; J. T. O'Neal; F. Li; M. Sammalkorpi; J. L. Lutkenhaus, 2018. *ACS Central Sci.*, 4(5), 638–644. Copyright (2018) American Chemical Society; each data point represents a single experiment. The line represents the fit of eqn (1) to all of the data in the plot.

suggesting distinct ion interactions at lower concentrations that transition to uniform bridging and ion pairing as salt concentration increases. Discussed later, these data later become normalized by ion pairing to reveal much better correlation.

3.5. Combined water and salt effects on the T_g of PDADMA/PSS PECs

As mentioned in the Introduction, our prior work reported a water-salt-T_g relationship, for which the T_g's of PDADMA–PSS PECs prepared in various NaCl concentrations collapsed into a single curve as described by eqn (1).[14] To examine the applicability of eqn (1) in divalent salt systems, we plotted Fig. 6, which shows $\ln\left(\frac{n_{H_2O}}{n_{\text{intrinsic ion pair}}}\right)$ vs. $\frac{1000}{T_g}$ for PECs made with MgCl$_2$, CaCl$_2$, and NaCl (as a control). $n_{\text{intrinsic ion pair}}$ was estimated from a charge balance, a mole balance, and the doping level. Here, $n_{\text{intrinsic ion pair}}$ was calculated from the expressions in eqn (5) to account for the bivalency of the magnesium or calcium ions and any remaining
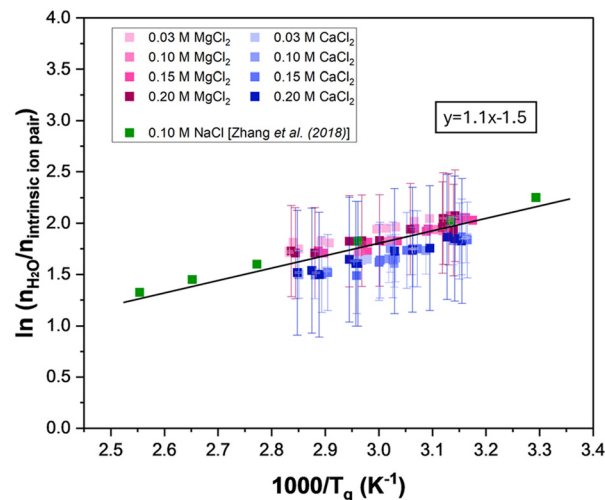
sodium ions. From this fit, we extract the Van't Hoff enthalpy, H_{VH}, following eqn (8):

$$\frac{d(\ln K)}{dT} = -\frac{\Delta H_{VH}}{R} \quad (8)$$

where K is the equilibrium constant, R is the gas constant, and T is the absolute temperature. Here, K represents the equilibrium between an intrinsic ion pair with and without an additional water molecule in its hydration shell.[33]

The impact of varying salt concentration (0.03–0.20 M) on the water-salt-T_g relationship for PDADMA–PSS PECs is shown in Fig. 6. Notably, there was a linear overlap consistent with all the salt types and concentrations examined, following the scaling of eqn (1).[14] As shown in Table S5 (ESI†), the slopes and y-intercepts were largely within error of each other. For example, the master curve for NaCl was characterized by a slope, intercept, and energy of 1.30, −1.98, and −10.8 kJ mol^{-1}, respectively.[14,64] This overlap indicates a strong connection between the T_g and the hydrogen bonding water network in the polyelectrolyte complexes, regardless of salt type or valency.

From Table S5 (ESI†), the Van't Hoff enthalpies for our PECs assembled in MgCl$_2$ and CaCl$_2$ at the concentrations 0.03–0.20 M averaged to 11.8 ± 2.1 kJ mol^{-1} and 10.1 ± 1.6 kJ mol^{-1}, respectively, which are within the range of the enthalpy associated with breaking one O–H···O unit (∼10.8 ± 2.5 kJ mol^{-1}, see ref. 65). The intercept of the linear fit is linked to the entropic contributions within the PEC. For the MgCl$_2$ and CaCl$_2$ systems, the intercepts are similar to the NaCl PEC system, with values of −2.1 ± 0.8 and −2.0 ± 0.6, respectively. From these values and their overlap, we deduce that introducing divalent counterions

does not significantly alter the entropic contribution, which is related to the y-intercept. In our prior work, the y-intercept varied between PEC systems (PDADMA–PSS *versus* PAH–PAA[14]) and for PEMs in different salts (KBr[34] *versus* NaCl). From Fig. 6, although the divalent salts induce localized structural changes such as bridging, the T_g behavior remains largely the same once intrinsic ion pairing and water content are taken into account.

4. Conclusions

This work compared the composition and thermal properties of PDADMA–PSS PECs assembled in and exposed to NaCl, CaCl$_2$, and MgCl$_2$ solutions at different salt concentrations (0.03 M to 0.20 M) using MDSC, NMR spectroscopy, and NAA. All PECs contained excess PDADMA, leading to higher doping levels in PDADMA (y^+) relative to PSS (y^-). As expected, y^- increased with salt concentration; however, y^+ varied nonmonotonically. With the addition of water, the T_g of the PEC decreased, following previously reports.[14] Interestingly, the effects of divalent salts on the T_g were more nuanced. At the same salt concentration, the T_g followed as 0.10 M NaCl > 0.10 M CaCl$_2$ > 0.10 M MgCl$_2$. This was explained by the ion-specific effects of the Hofmeister ion series and ionic properties, such as the hydration number. The effect of the ionic strength and salt concentration of CaCl$_2$ and MgCl$_2$ on the PEC's T_g was also studied. At low divalent salt concentrations, chelation or bridging effects were indirectly observed in our system (*i.e.*, PSS–Ca–PSS or PSS–Mg–PSS). At high divalent salt concentrations, salting in become more influential. This transition occurs at a lower concentration for CaCl$_2$-PECs due to Ca^{2+} having a higher affinity for PSS than Mg^{2+}.

This work also explored the water-salt-T_g relationship for PDADMA–PSS PECs in the presence of the salts with divalent cations. Prior work from our group established distinct master curves for PDADMA–PSS PECs, PAH–PAA PECs, and PEMs prepared with NaCl, but not divalent salts. Here, for CaCl$_2$-PECs and MgCl$_2$-PECs there was an overlay with the master curve regarding the slope, intercept, and energy within error to the values for monovalent NaCl-PECs. The $\frac{1000}{T_g} \sim \ln\left(n_{\text{H}_2\text{O}}/n_{\text{intrinsic ion pair}}\right)$ relationship was found to be general regardless of the salt used in assembly, further highlighting the intricacies of the polyelectrolyte microenvironment. In total, despite bridging and chelation effects brought about by divalent cations, the structural relaxation of the PEC remains the same.

Abbreviations

PAA	Poly(acrylic acid)
PAH	Poly(allylamine hydrochloride)
PDADMA	Poly(diallydimethylammonium)
PSS	Poly(styrenesulfonate)
D$_2$O	Deuterium oxide
KBr	Potassium bromide
NaCl	Sodium chloride
CaCl$_2$	Calcium chloride
MgCl$_2$	Magnesium chloride
PE	Polyelectrolyte
PECs	Polyelectrolyte complexes
DSC	Differential scanning calorimetry
MDSC	Modulated differential scanning calorimetry
NAA	Neutron activation analysis
T_g	Glass transition temperature
$n_{\text{H}_2\text{O}}$	Number of water molecules
$n_{\text{intrinsic ion pairs}}$	Number of intrinsic ion pairs
K	Equilibrium constant
$n_{\text{PSS–Na}}$	Moles of PSS–sodium interactions
n_{Na}	Moles of sodium
$n_{\text{PSS–PDADMA}}$	Moles of PSS–PDADMA interactions
n_{S}	Moles of sulfur
$n_{\text{PDADMA–Cl}}$	Moles of PDADMA–chlorine interactions
n_{Cl}	Moles of chlorine
ΔH	Enthalpy change associated with insertion of water molecule
R	Universal gas constant
A_{aromatic}	Area of aromatic hydrogens
$A_{\text{aliphatic}}$	Area of aliphatic hydrogens
y^+	Doping level for PDADMA
y^-	Doping level for PSS
[anion]	Concentration of negative counterions in PECs
[cation]	Concentration of positive counterions in PECs
[PSS]	Concentration of PSS
[PDADMA]	Concentration of PDADMA

Author contributions

T. B. and J. L. contributed to the design and implementation of the research, to the analysis of the results and to the writing of the manuscript. T. B. carried out the experiments. S. L. and C. I. contributed conceptually to the experimental design and editing the manuscript.

Data availability

The data supporting this article have been included as part of the ESI.†

Conflicts of interest

There are no conflicts of interest to declare.

Acknowledgements

References

1 J. K. Bediako, E. S. M. Mouele, Y. El Ouardi and E. Repo, Saloplastics and the polyelectrolyte complex continuum: Advances, challenges and prospects, *Chem. Eng. J.*, 2023, **462**, 142322.

2 G. Decher, Fuzzy Nanoassemblies: Toward Layered Polymeric Multicomposites, *Science*, 1997, **277**(5330), 1232–1237.

3 L.-M. Petrila, F. Bucatariu, M. Mihai and C. Teodosiu, Polyelectrolyte Multilayers: An Overview on Fabrication, Properties, and Biomedical and Environmental Applications, *Materials*, 2021, **14**, 4152.

4 S. Chen and Z.-G. Wang, Driving force and pathway in polyelectrolyte complex coacervation, *Proc. Natl. Acad. Sci. U. S. A.*, 2022, **119**(36), e2209975119.

5 V. Sharma and A. Sundaramurthy, Multilayer capsules made of weak polyelectrolytes: a review on the preparation, functionalization and applications in drug delivery, *Beilstein J. Nanotechnol.*, 2020, **11**, 508–532.

6 T.-H. Dao, T.-Q.-M. Vu, N.-T. Nguyen, T.-T. Pham, T.-L. Nguyen, S.-I. Yusa and T.-D. Pham, Adsorption Characteristics of Synthesized Polyelectrolytes onto Alumina Nanoparticles and their Application in Antibiotic Removal, *Langmuir*, 2020, **36**(43), 13001–13011.

7 M. Criado-Gonzalez, C. Mijangos and R. Hernández, Polyelectrolyte Multilayer Films Based on Natural Polymers: From Fundamentals to Bio-Applications, *Polymers*, 2021, **13**, 2254.

8 I. Dogaris, I. Pylypchuk, G. Henriksson and A. Abbadessa, Polyelectrolyte complexes based on a novel and sustainable hemicellulose-rich lignosulphonate for drug delivery applications, *Drug Delivery Transl. Res.*, 2024, **14**, 3452–3466.

9 B. Peng, Q. Lyu, Y. Gao, M. Li, G. Xie, Z. Xie, H. Zhang, J. Ren, J. Zhu, L. Zhang and P. Wang, Composite Polyelectrolyte Photothermal Hydrogel with Anti-biofouling and Antibacterial Properties for the Real-World Application of Solar Steam Generation, *ACS Appl. Mater. Interfaces*, 2022, **14**(14), 16546–16557.

10 L. Fernández-Peña, E. Guzmán, C. Fernández-Pérez, I. Barba-Nieto, F. Ortega, F. Leonforte, R. G. Rubio and G. S. Luengo, Study of the Dilution-Induced Deposition of Concentrated Mixtures of Polyelectrolytes and Surfactants, *Polymers*, 2022, **14**, 1335.

11 M. Jia, L. Luo and M. Rolandi, Correlating Ionic Conductivity and Microstructure in Polyelectrolyte Hydrogels for Bioelectronic Devices, *Macromol. Rapid Commun.*, 2022, **43**(6), 2100687.

12 J. Fu, R. L. Abbett, H. M. Fares and J. B. Schlenoff, Water and the Glass Transition Temperature in a Polyelectrolyte Complex, *ACS Macro Lett.*, 2017, **6**(10), 1114–1118.

13 Y. Zhang, F. Li, L. D. Valenzuela, M. Sammalkorpi and J. L. Lutkenhaus, Effect of Water on the Thermal Transition Observed in Poly(allylamine hydrochloride)–Poly(acrylic acid) Complexes, *Macromolecules*, 2016, **49**(19), 7563–7570.

14 Y. Zhang, P. Batys, J. T. O'Neal, F. Li, M. Sammalkorpi and J. L. Lutkenhaus, Molecular Origin of the Glass Transition in Polyelectrolyte Assemblies, *ACS Cent. Sci.*, 2018, **4**(5), 638–644.

15 R. Chollakup, W. Smitthipong, C. D. Eisenbach and M. Tirrell, Phase Behavior and Coacervation of Aqueous Poly(acrylic acid)–Poly(allylamine) Solutions, *Macromolecules*, 2010, **43**(5), 2518–2528.

16 J. Choi and M. F. Rubner, Influence of the Degree of Ionization on Weak Polyelectrolyte Multilayer Assembly, *Macromolecules*, 2005, **38**(1), 116–124.

17 R. G. Larson, Y. Liu and H. Li, Linear viscoelasticity and time-temperature-salt and other superpositions in polyelectrolyte coacervates, *J. Rheol.*, 2021, **65**(1), 77–102.

18 A. Sill, P. Nestler, A. Azinfar and C. A. Helm, Tailorable Polyanion Diffusion Coefficient in LbL Films: The Role of Polycation Molecular Weight and Polymer Conformation, *Macromolecules*, 2019, **52**(22), 9045–9052.

19 O. Soltwedel, P. Nestler, H.-G. Neumann, M. Paßvogel, R. Köhler and C. A. Helm, Influence of Polycation (PDAD-MAC) Weight on Vertical Diffusion within Polyelectrolyte Multilayers during Film Formation and Postpreparation Treatment, *Macromolecules*, 2012, **45**(19), 7995–8004.

20 E. Tsuchida, Formation of Polyelectrolyte Complexes and Their Structures, *J. Macromol. Sci., Part A: Pure Appl. Chem.*, 1994, **31**(1), 1–15.

21 K. Abe, M. Koide and E. Tsuchida, Selective Complexation of Macromolecules, *Macromolecules*, 1977, **10**(6), 1259–1264.

22 J. Fu, H. M. Fares and J. B. Schlenoff, Ion-pairing strength in polyelectrolyte complexes, *Macromolecules*, 2017, **50**(3), 1066–1074.

23 E. Guzmán, A. Maestro, F. Ortega and R. G. Rubio, Association of oppositely charged polyelectrolyte and surfactant in solution: equilibrium and nonequilibrium features, *J. Phys.: Condens. Matter*, 2023, **35**(32), 323001.

24 Z. Ye, S. Sun and P. Wu, Distinct Cation–Anion Interactions in the UCST and LCST Behavior of Polyelectrolyte Complex Aqueous Solutions, *ACS Macro Lett.*, 2020, **9**(7), 974–979.

25 Q. Wang and J. B. Schlenoff, The Polyelectrolyte Complex/Coacervate Continuum, *Macromolecules*, 2014, **47**(9), 3108–3116.

26 S. Meng, Y. Liu, J. Yeo, J. M. Ting and M. V. Tirrell, Effect of mixed solvents on polyelectrolyte complexes with salt, *Colloid Polym. Sci.*, 2020, **298**(7), 887–894.

27 A. S. Michaels, Polyelectrolyte Complexes, *Ind. Eng. Chem.*, 1965, **57**(10), 32–40.

28 X. Lyu, B. Clark and A. M. Peterson, Thermal transitions in and structures of dried polyelectrolytes and polyelectrolyte complexes, *J. Polym. Sci., Part B: Polym. Phys.*, 2017, **55**(8), 684–691.

29 S. De, C. Cramer and M. Schönhoff, Humidity Dependence of the Ionic Conductivity of Polyelectrolyte Complexes, *Macromolecules*, 2011, **44**(22), 8936–8943.

30 C. I. Eneh, T. Kastinen, S. Oka, P. Batys, M. Sammalkorpi and J. L. Lutkenhaus, Quantification of Water–Ion Pair Interactions in Polyelectrolyte Multilayers Using a Quartz

Crystal Microbalance Method, *ACS Polym. Au*, 2022, **2**(4), 287–298.

31 R. Zhang, Y. Zhang, H. S. Antila, J. L. Lutkenhaus and M. Sammalkorpi, Role of Salt and Water in the Plasticization of PDAC/PSS Polyelectrolyte Assemblies, *J. Phys. Chem. B*, 2017, **121**(1), 322–333.

32 Y. Zhang, E. Yildirim, H. S. Antila, L. D. Valenzuela, M. Sammalkorpi and J. L. Lutkenhaus, The influence of ionic strength and mixing ratio on the colloidal stability of PDAC/PSS polyelectrolyte complexes, *Soft Matter*, 2015, **11**(37), 7392–7401.

33 H. Li, S. M. Lalwani, C. I. Eneh, T. Braide, P. Batys, M. Sammalkorpi and J. L. Lutkenhaus, A Perspective on the Glass Transition and the Dynamics of Polyelectrolyte Multilayers and Complexes, *Langmuir*, 2023, **39**(42), 14823–14839.

34 J. T. O'Neal, K. G. Wilcox, Y. Zhang, I. M. George and J. L. Lutkenhaus, Comparison of KBr and NaCl effects on the glass transition temperature of hydrated layer-by-layer assemblies, *J. Chem. Phys.*, 2018, **149**(16), 163317.

35 S. M. Lalwani, K. Hellikson, P. Batys and J. L. Lutkenhaus, Counter Anion Type Influences the Glass Transition Temperature of Polyelectrolyte Complexes, *Macromolecules*, 2024, **57**(10), 4695–4705.

36 J. Yu, N. Jackson, X. Xu, Y. Morgenstern, Y. Kaufman, M. Ruths, J. De Pablo and M. Tirrell, Multivalent counterions diminish the lubricity of polyelectrolyte brushes, *Science*, 2018, **360**(6396), 1434–1438.

37 J. Yu, J. Mao, G. Yuan, S. Satija, Z. Jiang, W. Chen and M. Tirrell, Structure of polyelectrolyte brushes in the presence of multivalent counterions, *Macromolecules*, 2016, **49**(15), 5609–5617.

38 J. Yu, N. E. Jackson, X. Xu, B. K. Brettmann, M. Ruths, J. J. De Pablo and M. Tirrell, Multivalent ions induce lateral structural inhomogeneities in polyelectrolyte brushes, *Sci. Adv.*, 2017, **3**(12), eaao1497.

39 D. Iyer, V. M. S. Syed and S. Srivastava, Influence of divalent ions on composition and viscoelasticity of polyelectrolyte complexes, *J. Polym. Sci.*, 2021, **59**(22), 2895–2904.

40 H. Dautzenberg and J. Kriz, Response of Polyelectrolyte Complexes to Subsequent Addition of Salts with Different Cations, *Langmuir*, 2003, **19**(13), 5204–5211.

41 A. E. Neitzel, G. X. De Hoe and M. V. Tirrell, Expanding the structural diversity of polyelectrolyte complexes and polyzwitterions, *Curr. Opin. Solid State Mater. Sci.*, 2021, **25**(2), 100897.

42 S. L. Perry, Y. Li, D. Priftis, L. Leon and M. Tirrell, The effect of salt on the complex coacervation of vinyl polyelectrolytes, *Polymers*, 2014, **6**(6), 1756–1772.

43 C. G. Sinn, R. Dimova and M. Antonietti, Isothermal Titration Calorimetry of the Polyelectrolyte/Water Interaction and Binding of Ca2 +: Effects Determining the Quality of Polymeric Scale Inhibitors, *Macromolecules*, 2004, **37**(9), 3444–3450.

44 M. Chen, K. Shafer-Peltier, S. J. Randtke and E. Peltier, Competitive association of cations with poly(sodium 4-styrenesulfonate) (PSS) and heavy metal removal from water by PSS-assisted ultrafiltration, *Chem. Eng. J.*, 2018, **344**, 155–164.

45 J. L. Pauley, Prediction of Cation-exchange Equilibria, *J. Am. Chem. Soc.*, 1954, **76**(5), 1422–1425.

46 I. Sabbagh and M. Delsanti, Solubility of highly charged anionic polyelectrolytes in presence of multivalent cations: Specific interaction effect, *Eur. Phys. J. E: Soft Matter Biol. Phys.*, 2000, **1**(1), 75–86.

47 J. Fu and J. B. Schlenoff, Driving Forces for Oppositely Charged Polyion Association in Aqueous Solutions: Enthalpic, Entropic, but Not Electrostatic, *J. Am. Chem. Soc.*, 2016, **138**(3), 980–990.

48 A. Jusufi, A.-P. Hynninen, M. Haataja and A. Z. Panagiotopoulos, Electrostatic Screening and Charge Correlation Effects in Micellization of Ionic Surfactants. The, *J. Phys. Chem. B*, 2009, **113**(18), 6314–6320.

49 E. Jordan, F. Roosen-Runge, S. Leibfarth, F. Zhang, M. Sztucki, A. Hildebrandt, O. Kohlbacher and F. Schreiber, Competing Salt Effects on Phase Behavior of Protein Solutions: Tailoring of Protein Interaction by the Binding of Multivalent Ions and Charge Screening, *J. Phys. Chem. B*, 2014, **118**(38), 11365–11374.

50 A. Kundagrami and M. Muthukumar, Theory of competitive counterion adsorption on flexible polyelectrolytes: Divalent salts, *J. Chem. Phys.*, 2008, **128**(24), 244901.

51 K. Sadman, Q. Wang, Y. Chen, B. Keshavarz, Z. Jiang and K. R. Shull, Influence of Hydrophobicity on Polyelectrolyte Complexation, *Macromolecules*, 2017, **50**(23), 9417–9426.

52 H. H. Hariri, A. M. Lehaf and J. B. Schlenoff, Mechanical Properties of Osmotically Stressed Polyelectrolyte Complexes and Multilayers: Water as a Plasticizer, *Macromolecules*, 2012, **45**(23), 9364–9372.

53 M. McCormick, R. N. Smith, R. Graf, C. J. Barrett, L. Reven and H. W. Spiess, NMR Studies of the Effect of Adsorbed Water on Polyelectrolyte Multilayer Films in the Solid State, *Macromolecules*, 2003, **36**(10), 3616–3625.

54 G. Wypych, *Handbook of plasticizers*, ChemTec Publishing, 2004.

55 E. Immergut and H. Mark, Platzer: Plasticization and Plasticizer Processes, 1965.

56 R. Tomaš, M. Bešter-Rogač and T. Jovanović, Viscosity B-coefficient for sodium chloride in aqueous mixtures of 1, 4-dioxane at different temperatures, *Acta Chim. Slov.*, 2015, **62**(3), 531–537.

57 Y. Marcus, *Ion Properties*, CRC Press, New York, 1997.

58 A. G. Volkov, S. Paula and D. W. Deamer, Two mechanisms of permeation of small neutral molecules and hydrated ions across phospholipid bilayers, *Bioelectrochem. Bioenerg.*, 1997, **42**(2), 153–160.

59 E. R. Nightingale, Phenomenological Theory of Ion Solvation. Effective Radii of Hydrated Ions, *J. Phys. Chem.*, 1959, **63**(9), 1381–1387.

60 M. P. Andersson and S. L. Stipp, Predicting hydration energies for multivalent ions, *J. Comput. Chem.*, 2014, **35**(28), 2070–2075.

61 Y. Marcus, A simple empirical model describing the thermodynamics of hydration of ions of widely varying charges, sizes, and shapes, *Biophys. Chem.*, 1994, **51**(2–3), 111–127.

62 J. Wei, D. A. Hoagland, G. Zhang and Z. Su, Effect of Divalent Counterions on Polyelectrolyte Multilayer Properties, *Macromolecules*, 2016, **49**(5), 1790–1797.

63 A. Glisman, S. Mantha, D. Yu, E. P. Wasserman, S. Backer and Z.-G. Wang, Multivalent Ion-Mediated Polyelectrolyte Association and Structure, *Macromolecules*, 2024, **57**(5), 1941–1949.

64 Y. Zhang, P. Batys, J. T. O'Neal, F. Li, M. Sammalkorpi and J. L. Lutkenhaus, Molecular Origin of the Glass Transition in Polyelectrolyte Assemblies, *ACS Cent. Sci.*, 2018, **4**(5), 638–644.

65 G. Walrafen, Raman spectral studies of HDO in H2O, *J. Chem. Phys.*, 1968, **48**(1), 244–251.